

Simulation of Coupled-Oscillator Feedback Systems Counteracting the Strong Head-Tail Effect in LEP

G. Sabbi

Abstract

A new technique aiming at the stabilization of the strong head-tail effect, based on the use of feedback oscillators coupled to the TMC modes, was proposed and tested in LEP. In this report, the results obtained by simulating the collective motion of the bunch in the presence of the new feedback using the multi-particle tracking program TRISIM will be presented, in order to better understand the physics of the system and to evaluate, for some of the possible configurations, the hardware specifications which would be required to obtain a 25% increase of the maximum bunch current with respect to the TMC threshold.

Geneva, Switzerland

January 1996

1 Introduction

A new feedback system counteracting the transverse mode coupling instability, based on the use of feedback oscillators coupled to the TMC modes, has been proposed by V. Danilov and E. Perevedentsev. Ref. [1] presents a rigorous and detailed description of this system: here only the main features will be outlined using a rather intuitive approach, to provide a framework for the following analysis.

The basic principle is to enforce a coupling between the coherent dipole mode $m=0$ and an artificial oscillator, modelled by the feedback hardware. This coupling provides a force which prevents the frequency of mode $m=0$ from shifting towards the synchrotron sideband $m=-1$, thus avoiding the onset of TMC.

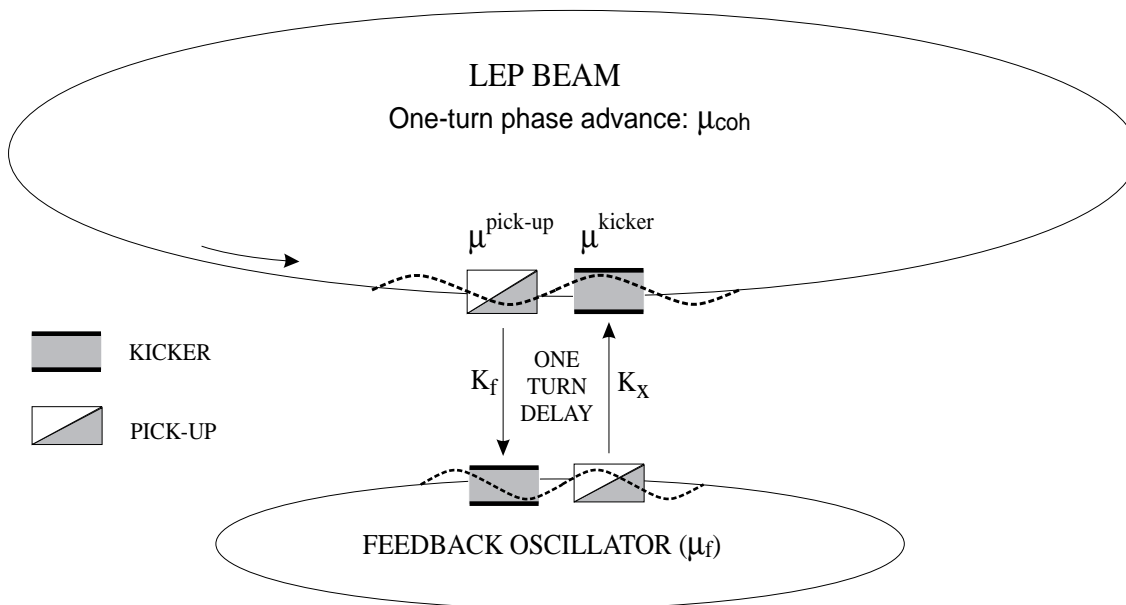


Figure 1: Basic configuration for the coupled-oscillator feedback system proposed by Danilov and Perevedentsev.

The basic configuration is illustrated in Fig. 1, where the artificial oscillator is represented as a charge rotating around a ring with the same revolution frequency and phase of the beam, and performing betatron oscillations with a one-turn phase advance μ_f : the motivation for this “bunch-like” representation of the oscillator will be clear from what follows. At each passage of the bunch through the feedback kicker, both the bunch and the feedback oscillator are applied corrections which have been computed from position measurements taken *at the previous turn*. At (ideally) the same time, the position of both the bunch and the feedback oscillator is measured, in order to compute the corrections which will be applied *at the following turn*. For this system, no timing problems arise as a whole revolution period is available to prepare the next correction after the bunch has passed through the kicker; for what concerns the feedback oscillator, the time needed to perform the calculations is negligible.

A simple example, reported in [1], shows how the configuration described can provide, with suitable choices of the (current dependent) oscillator phase advance per turn and of the feedback

gain, a coupled system in which the eigenfrequencies of the normal modes do not depend on current. For this purpose, it is sufficient to write the one-turn transfer matrix for the dynamical variables (position and slope) of the two coupled oscillators, representing a mutual kick followed by a free oscillation: assuming a linear phase shift with current, $\mu_{coh} = \mu_\beta + \alpha I_b$, one obtains:

$$M = \begin{bmatrix} \cos(\mu_\beta + \alpha I_b) & \sin(\mu_\beta + \alpha I_b) & 0 & 0 \\ -\sin(\mu_\beta + \alpha I_b) & \cos(\mu_\beta + \alpha I_b) & 0 & 0 \\ 0 & 0 & \cos(\mu_f) & \sin(\mu_f) \\ 0 & 0 & -\sin(\mu_f) & \cos(\mu_f) \end{bmatrix} \begin{bmatrix} 1 & 0 & 0 & 0 \\ 0 & 1 & K_x & 0 \\ 0 & 0 & 1 & 0 \\ K_f & 0 & 0 & 1 \end{bmatrix} \quad (1)$$

If the feedback parameters¹ μ_f and K_x are solutions of the equations:

$$\cos(\mu_f) = 2 \cos(\mu_\beta) - \cos(\mu_\beta + \alpha I_b) \quad (2)$$

$$K_x K_f = -\frac{[\cos(\mu_\beta) - \cos(\mu_\beta + \alpha I_b)]^2}{\sin(\mu_f) \sin(\mu_\beta + \alpha I_b)} \quad (3)$$

then the eigenvalues of the matrix M (and hence the mode frequencies of the coupled system bunch+oscillator) do not depend on current [1] and stay equal to the zero-current tune μ_β , which means that the coherent tune shift leading to transverse mode coupling is virtually eliminated.

In this representation of the feedback system, the oscillator could be regarded as a mirror image of the bunch: in fact, according to equation 2, for increasing currents μ_f shifts upwards as μ_{coh} shifts downwards (since $\alpha < 0$), and the two stay approximately symmetric with respect to the zero-current betatron phase advance μ_β . The phase advances per turn μ_{coh} and μ_f are those corresponding to the uncoupled system ($K_x=0$); then, as the gain is raised up to its nominal value (given by equation 3), an attractive force is established between the coherent mode $m=0$ and the oscillator, so that their tunes get closer to each other, until they merge at a value equal to Q_β . This way of representing the feedback operation is quite useful, as it reveals that the settings calculated according to equations 2 and 3 are just one possible solution, aiming at a coupled system with current-independent mode frequencies; however, different strategies for choosing the feedback settings can also be envisaged, which may prove to be more effective in providing the maximum current gain. In fact, it should be noted that the new ‘‘oscillator’’ mode introduced in the transverse spectrum of the bunch by the feedback system may be responsible for the onset of instabilities due to its coupling with other coherent modes. Although the conditions leading to dangerous coupling can be predicted by more sophisticated theoretical models [1], simulation can be of great help in the *definition of an optimal strategy for the choice of the feedback settings*, which will be a first important task of the present study.

For what concerns the practical layout of the system, in case a pick-up is not available at the location of the feedback kicker (as for the system presently implemented in LEP), the position of the bunch at the kicker can be calculated using the measurements taken by two pick-ups placed upstream:

$$z_{kicker} = g_1 z_{pu1} + g_2 z_{pu2} \quad (4)$$

¹Since the gains K_x and K_f only appear as a product in equation 3, it is convenient to set $K_f=1$ and to retain K_x as the only independent parameter.

where g_1 and g_2 are functions of the betatron phase advances between the pick-ups and the kicker. The additional time delay in obtaining the input value for the calculation of the kick which must be applied to the feedback oscillator does not create problems, as the oscillator can easily catch up with the beam in a fraction of the revolution period. However, it is also important to ensure that the position of the bunch at the “virtual” pick-up can be computed with sufficient accuracy. *The evaluation of the sensitivity of the feedback performance with respect to errors in the calculation of the bunch position will be a second important aspect of the present study.*

This work is a continuation of simulation studies carried out in 1993-94, which played an essential role in the feedback development: although a detail report of those results was not issued, the main conclusions were reported by D. Brandt in [2], together with the results of the experiments carried out in the same period. The present report is organized as follows: in section 2, a brief description of the machine model and of the machine settings which have been used for the simulations will be given; then the behaviour of the coupled-oscillator feedback will be analysed in section 3 assuming ideal conditions (that is with no limitations either in the accuracy of the pick-up system or in the kick strength), in order to study the beam dynamics in the presence of feedback, and to optimize the settings for the maximum current gain. In section 4, the effect of hardware limitations on the feedback performance will be studied, in order to estimate the hardware specifications which would be required in order to achieve a 25% increase of the maximum bunch current, with the machine settings which have been selected for the present study and using a configuration of the coupled-oscillator feedback in which *an attractive force is established between the coherent mode $m=0$ and the oscillator*. In section 5, an alternative configuration in which *a repulsive force is established between the coherent mode $m=0$ and the oscillator* is considered, and it will be shown that in this mode of operation a relaxation of some hardware constraints is possible. Finally, a synthesis of the results which have been obtained will be given in section 6.

2 Machine model

The geometry of LEP has been modelled by a ring divided into 8 sectors, each one starting with a point-like element (labeled as E1 ... E8), followed by an arc section in which the motion is assumed linear. This machine representation is illustrated in Fig. 2: the element E1, placed at the position conventionally indicated as “start LEP” (IP1), represents a pick-up which collects, at each turn, the relevant bunch data; the elements E2 and E7 represent the LEP RF stations in IP2 and IP6; each of the elements E2 and E7 also accounts for one fourth of LEP impedance, while E6 and E8 account for the remaining impedance; the elements E3 and E4 represent the feedback pick-ups, while the element E5 represents the feedback kicker.

The collective motion of a set of macroparticles in this virtual machine has been simulated, in a 2D longitudinal-vertical plane, using the multi-particle tracking program TRISIM [3]: the beam dynamics includes synchrotron radiation loss, radiation damping, quantum excitation, sinusoidal RF, and chromaticity. The wakefield effects, which depend on the particle distribution, are represented as kicks, lumped at the elements E2, E6, E7, E8. A detailed discussion concerning the equations of motion, the wakefield representation technique, and the efficiency of this model in representing the real machine can be found in [4].

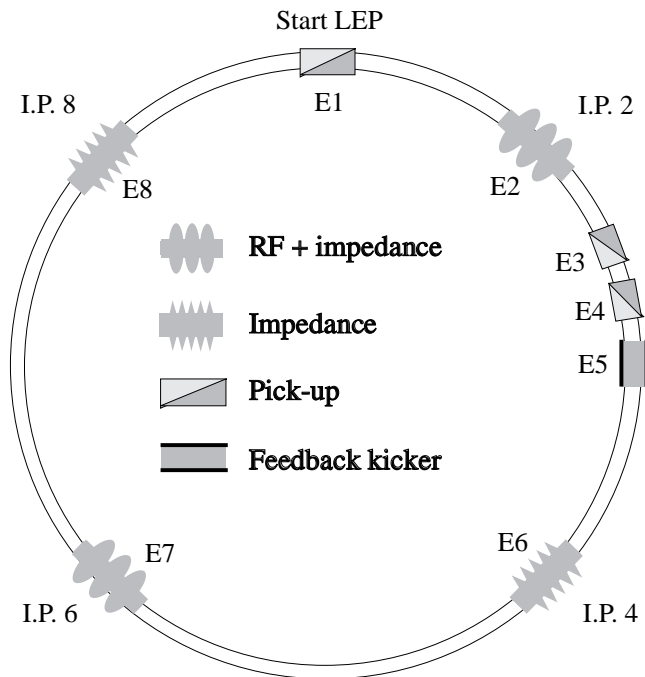


Figure 2: The LEP machine model

For what concerns the impedance model, several elementary structures are considered: one cell of the copper cavity, a four-cell superconducting cavity, an electrostatic vertical separator, the different bellows and tapers which connect these structures to the vacuum chamber, and a shielded bellows for vacuum chamber interconnections in the arcs. For each structure, the wake potential for a reference (basis function) distribution, having a triangular longitudinal shape and a multipolar dependence on the azimuth, has been computed using the electromagnetic mesh code ABCI [5]. The reference wake potentials so-obtained have then been combined in “effective wakes” for the point-like elements, by taking into account the number of structures in each impedance class, and the average values of the (vertical) β function for each class. For the present study, the optics functions corresponding to the LEP $90^\circ/60^\circ$ (1994) lattice were chosen: the momentum compaction factor is $\alpha_c = 1.86 \cdot 10^{-4}$, while the average values of the β function at each impedance class are reported in table 1, together with the number of structures, corresponding to the LEP status during the 1994 run. A vertical β of 56.4 m (equal to the average β in the ring) has been assumed at both the feedback pick-ups and at the kicker.

More details about the impedance model and the calculation of the reference wakes are provided in [4], where a discussion concerning the possibility of representing the effect of different structures as an “effective wake” lumped at a point-like element can also be found.

For what concerns the other beam parameters, table 2 reports the values of the zero-current energy spread, of the radiation energy loss, and of the radiation damping time, for nominal excitation of the wiggler magnets [6]. All the calculations have been carried out assuming zero chromaticity.

The number of macroparticles has been chosen according to the criteria formulated in [4]: a few thousands particles have been used in most cases. The simulations have been carried out for a number of turns corresponding to several damping times, the output data (equilibrium

Structure	N	$\langle \beta_y \rangle$ [m]
Copper cavity cell	600	40.6
Four cell SC cavity	20	51.3
ZL tank & electrodes	36	66.4
Separator tapers & bellows	47	56.1
Straight section bellows (L)	128	40.6
Straight section bellows (S)	160	40.6
SC module taper	5	51.3
Shielded bellows (arc)	2668	84.8

Table 1: Impedance model of LEP: the elementary structures which have been taken into account, their number, and the average values of the (vertical) β function are reported. The average β function values at the RF cavities and in the arcs have been computed by A. Verdier.

Wiggler Excitation		Radiation	Energy	Energy
Damping	Polarization	loss/turn	spread	damping time
A	A	MeV	MeV	s
520	500	14.97	36.4	0.119

Table 2: Beam parameters for nominal wiggler currents [6].

values, mode spectra) were calculated only over the last damping time.

In order to estimate the gain which can be provided by the feedback system with respect to the maximum bunch currents which can be achieved without feedback, the machine conditions which have been selected for the present study are those of a typical high-current experiment at LEP, that is with both damping and polarization wigglers excited, and with a rather high synchrotron tune ($Q_s=0.108$). First, the TMC limit without feedback has been calculated by simulating an accumulation process in steps of $20\mu\text{A}$, and the last stable bunch current has been found to be equal to 0.78 mA: figure 3 reports a summary of the simulation results for $I_b=0.8$ mA, where the TMC limit is reached. An experiment carried out with similar machine settings during the 1993 run yielded a maximum bunch current of 0.73 mA. For what concerns the 1994 run, no experimental data taken in the same conditions are available; however, the 1993 data may be regarded as essentially correct, with some possible reduction due to slightly higher values of the average β function in the 1994 optics, and due to the installation of a few more elements contributing to the machine impedance (separators, SC cavities). This comparison indicates that the threshold current obtained by simulation is overestimated by a factor of about 10-15%: this discrepancy is believed to be a consequence of an underestimation of the LEP impedance in the model of table 1, due to several contributions which have not been taken into account [4, 7].

INPUT FILE NAME qv24nf (part 3) RUN DATE 24/ 8/ 95 TIME 16. 10. 12

Distributions are approximated by linear interpolation (20 ps step)
Longitudinal wake switched ON – Transverse wake switched ON

Number of particles 1000 Damping time (s) 0.119 Beam energy (GeV) 20
Number of turns 3000 Energy spread (MeV) 36.4 Radiation loss (MeV) 14.97

Bunch current (mA)	0.8	Betatron tune	76.24
Total RF Voltage (MV)	250	Synchrotron tune	0.108

FEEDBACK SETTINGS Phase advance between (virtual) pick-up and kicker (DEG) 0
RMS pick-up noise (microns) 0 Number of kickers 1

FEEDBACK IS SWITCHED OFF

Equilibrium values (averaged over 1000 turns)

Bunch center (ps) -72.517 Bunch length (ps) 42.819 Bunch width (mm) 0.353
Mean energy (MeV) -5.023 Energy spread (MeV) 37.577 Total losses (MeV) 39.948

Total CPU time (s) 989.187 Time for wake calculation (s) 65.226

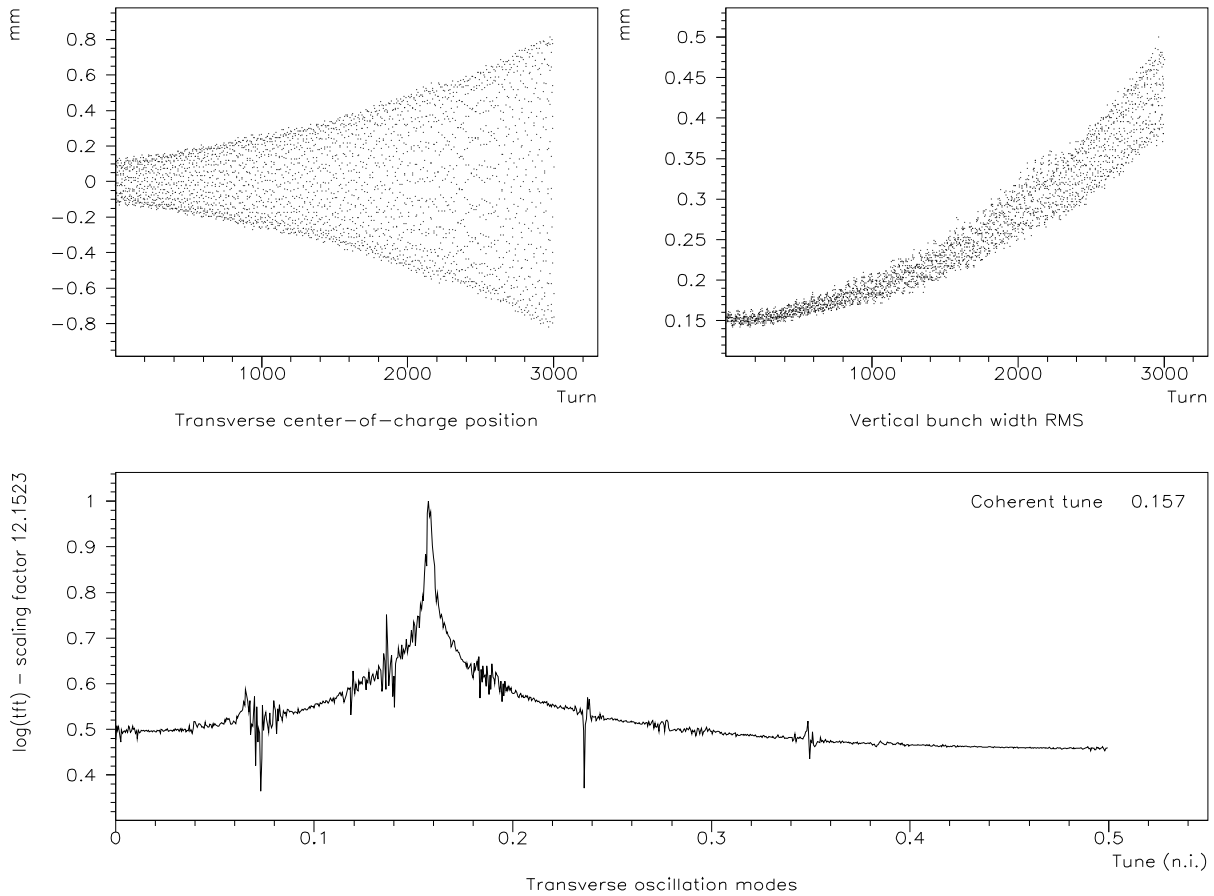


Figure 3: TMC threshold (feedback off).

3 Feedback performance in ideal conditions

This section will be devoted to the study of the behaviour of the coupled-oscillator feedback system assuming ideal conditions, that is with no limitations either in the accuracy of the measurement of the bunch position or in the kick strength. It should be noted, however, that some fluctuations in the center-of-charge position are always present in the simulation, due to a residual effect of quantum excitation when a relatively small number of macroparticles is used. In order to estimate the size of this effect, the vertical position of the center of charge at the feedback kicker has been calculated at each turn by averaging over the vertical positions of all macroparticles, and compared to the value calculated using equation 4: the maximum and RMS deviations were checked using several different cases and found to be rather small, so that the results presented in what follows can still be considered to correspond to “ideal” when compared to what can be achieved by the hardware: with 500 macroparticles, the RMS error is already about 10^{-3} of the amplitude of the center-of charge oscillation, and further decreases when a higher number of macroparticles is used.

3.1 Compensation of the coherent detuning

In order to verify the capability of the feedback system to compensate the coherent detuning of mode $m=0$, a study of the vertical mode spectrum as a function of the feedback gain was carried out for a fixed bunch current $I_b=0.8$ mA, slightly above the maximum bunch current without feedback. The average detuning rate with current, calculated on the basis of the results obtained with feedback switched off and $Q_\beta=76.24$ (figure 3), is $\alpha=-104\text{A}^{-1}$. According to equations 2 and 3 the feedback settings are then $\mu_f=2.01$ (corresponding to an oscillator tune $Q_f=0.32$), $K_x=-0.0226\text{m}^{-1}$.

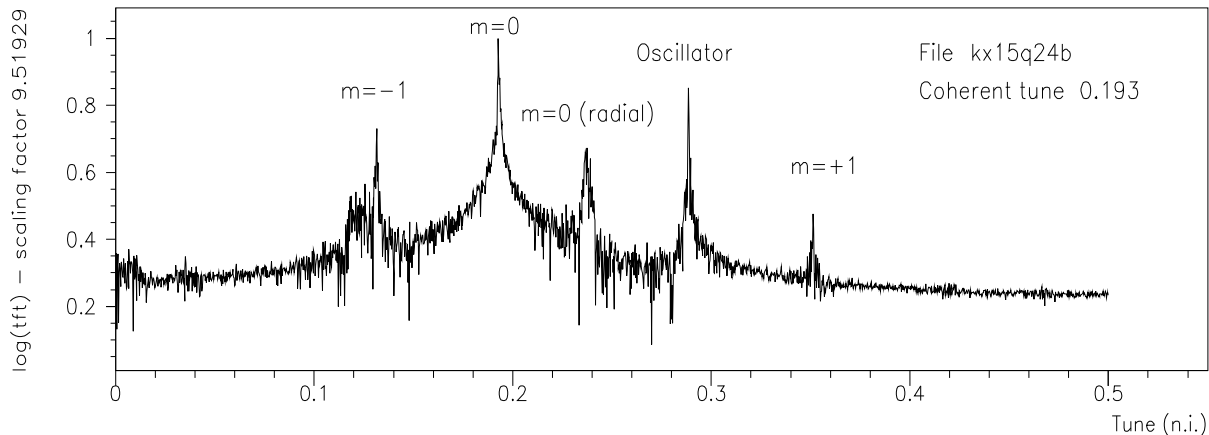


Figure 4: Transverse mode spectrum with feedback on: $I_b=0.8$ mA, ($Q_\beta=76.24$, $Q_f=0.32$, $K_x=-0.015\text{m}^{-1}$).

Figure 4 shows the transverse mode spectrum for $K_x=-0.015\text{m}^{-1}$ ($\approx 65\%$ of the nominal value): as can be seen, the coherent tune (indicated as “ $m=0$ ”) has been shifted back to 0.193 (+0.043 as compared to the case without feedback, figure 3). The new mode related to the feedback oscillator is also clearly visible at a tune of 0.288: the detuning of this mode due to the feedback coupling is then -0.032. The peak labelled as “ $m=0$ (radial)” corresponds to a cluster

of modes belonging to the $m=0$ azimuthal number (as the mode indicated as “ $m=0$ ”), but with higher-order radial dependence: they have been identified by comparing their behaviour with that observed for the eigenvalues of the mapping matrix of a beam whose longitudinal phase space has been divided into rings, each one with a given value of the synchrotron oscillation amplitude [1]. The smaller peaks which can be observed in the lower part of the spectrum, on the left of the synchrotron sideband $m=-1$, will be analyzed in detail in section 3.2 and will be shown to correspond to the higher-order modes $m=-2$, $m=-3$ (reflected).

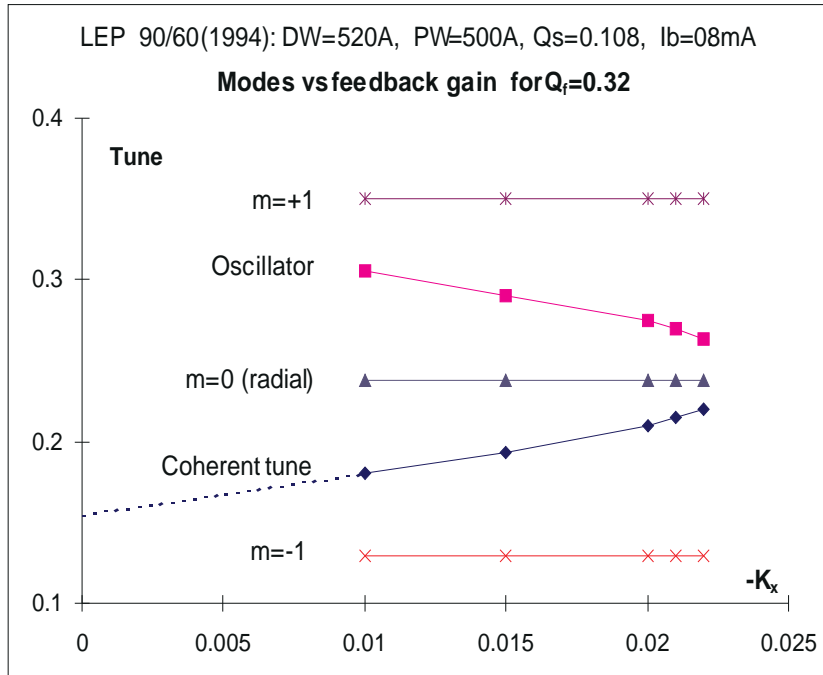


Figure 5: Compensation of the coherent detuning by the coupled-oscillator feedback system. $Q_\beta=76.24$, $Q_f=0.32$.

The curves reported in figure 5 have been obtained by calculating the tunes of the transverse modes for increasing values of the feedback gain K_x : as can be seen, the coherent tune can be shifted back to a value $Q_{coh}=0.22$, obtained with a feedback gain $K_x=-0.022 \text{ m}^{-1}$ (97% of the nominal value). The average detuning of the coherent dipole mode with current is then reduced from -104 A^{-1} to -25 A^{-1} , demonstrating that the feedback system works basically as predicted by theory; however, a further increase of the feedback gain leads to beam loss. In order to find the optimal strategy for the choice of the feedback settings, the instabilities which can occur when the feedback system is switched on will be further investigated in section 3.2 keeping a bunch current of 0.8 mA, before addressing the question of the maximum current gain which can be achieved. These instabilities can generally be predicted also by theory, although some of the effects have been successfully incorporated in the theoretical model only after having been observed in simulation [2].

3.2 Transverse instabilities in operation with feedback

In order to identify the instabilities which can occur when the feedback system is on, the machine and feedback settings have been chosen such as to selectively provide coupling between two

modes, while all the other modes are kept clear of each other. This condition is not satisfied in the case of the beam loss occurring for $|K_x| > 0.022$ in figure 5, where three modes are approaching each other at the same time.

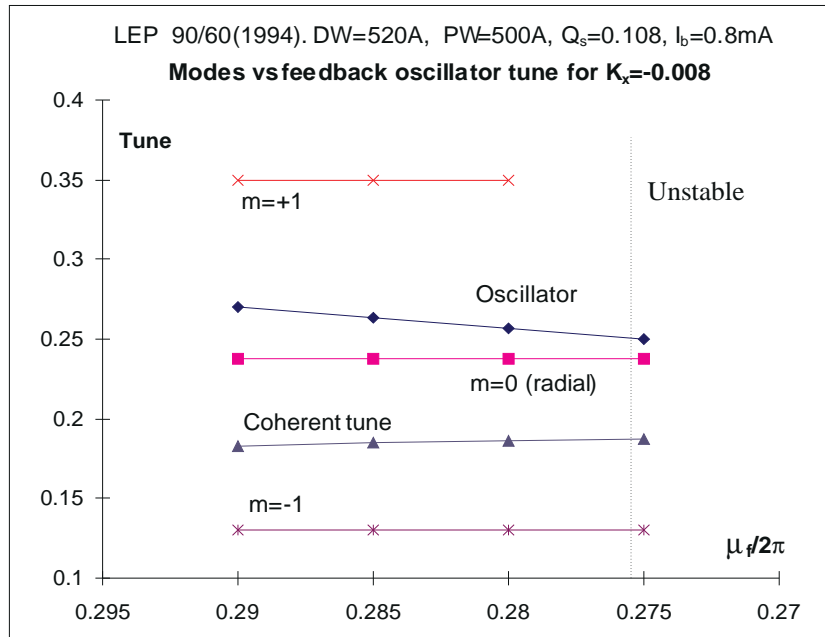


Figure 6: Instability due to coupling between the radial $m=0$ mode and the oscillator mode. For $\mu_f/2\pi=0.275$, a beam loss is observed, but since the growth rate of the instability is rather low it is still possible to compute the mode spectrum.

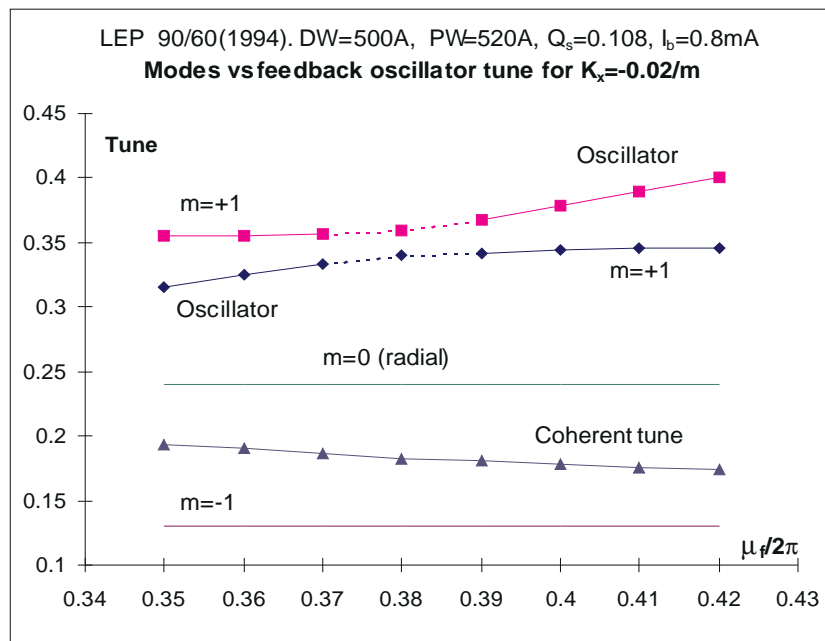


Figure 7: Interaction between the oscillator mode and the synchrotron sideband $m=+1$.

In the first calculation (figure 6), an instability due to coupling between the oscillator mode and the $m=0$ radial mode is found by letting the oscillator tune decrease until the two modes merge. Hence, the feedback settings will have to be chosen such as to keep the tune of the oscillator mode sufficiently away from that of the radial $m=0$ mode. However, no instability arises due to coupling between the oscillator mode and mode $m=+1$, as predicted by theory [1] and confirmed by the simulation results reported in figure 7, where the two modes can be observed exchanging their roles without merging their frequencies.

Figure 8 presents the results of a calculation aiming at obtaining the maximum compensation of the coherent tune shift of mode $m=0$. For this purpose, a high oscillator tune $Q_f=0.45$ was chosen, in order to avoid coupling of the oscillator mode with the radial $m=0$ mode.

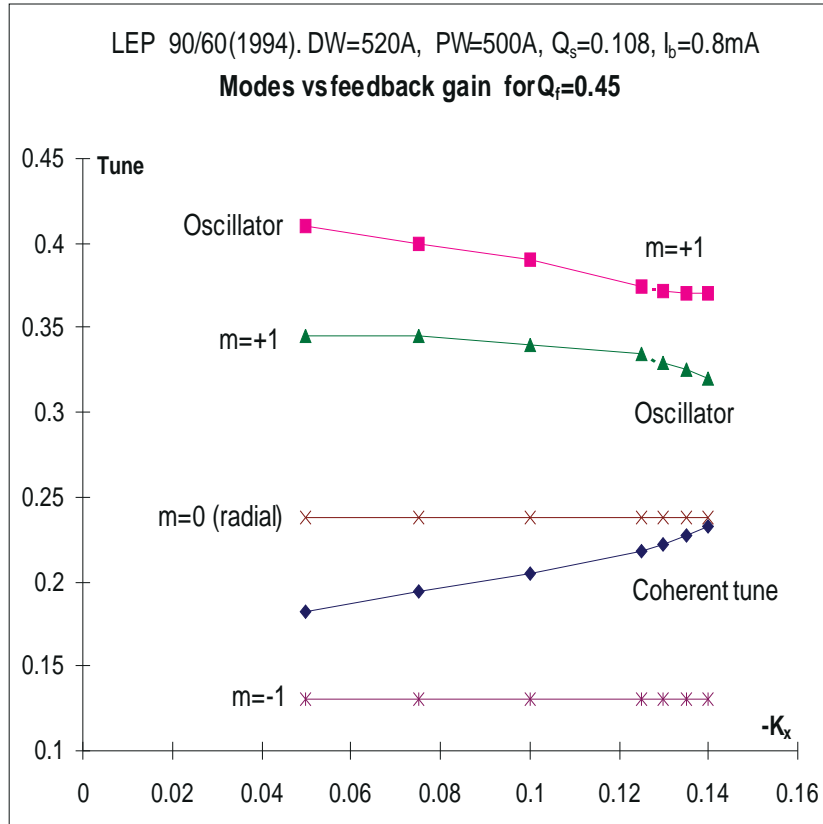


Figure 8: Compensation of the coherent detuning with $Q_f=0.45$.

As can be seen, the coherent $m=0$ mode can be shifted to a higher position with respect to the case with $Q_f=0.32$, and for $K_x=-0.14$ reaches a value of 0.231, very close to its zero-current value of 0.24: the corresponding mode spectrum is shown in figure 9. However, for higher values of the feedback gain again an instability occurs, which sets an upper limit to the maximum tune compensation which can be obtained by the feedback system.

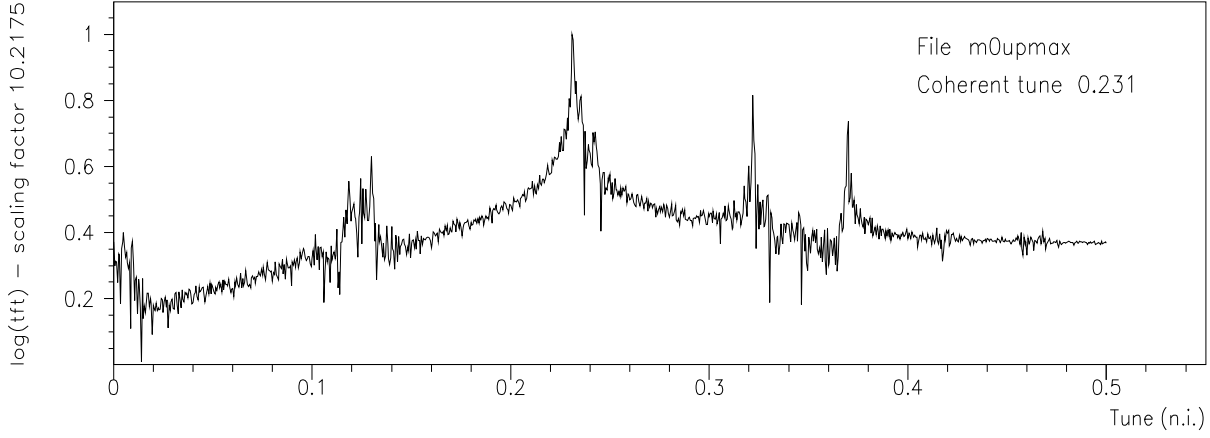


Figure 9: Transverse mode spectrum with feedback on and high oscillator tune: $I_b=0.8$ mA, $Q_f=0.45$, $K_x=-0.14\text{m}^{-1}$.

The last point in this section is devoted to the study of the instabilities due to coupling between mode $m=0$ and higher order (reflected) modes [9]. For this purpose, a scan of the zero-current tune Q_β from 0.24 down to 0.2 was carried out; at the same time, the oscillator tune was decreased from $Q_f=0.32$ to $Q_f=0.28$. The feedback gain K_x was equal to -0.15m^{-1} . In figure 10 the transverse mode spectrum for $Q_\beta=0.215$ is reported: here mode -3 is clearly shown between mode 0 and mode -1. A second important feature which is worth noting is that several azimuthal modes are split in clusters due to the different detuning experienced by the different radial components.

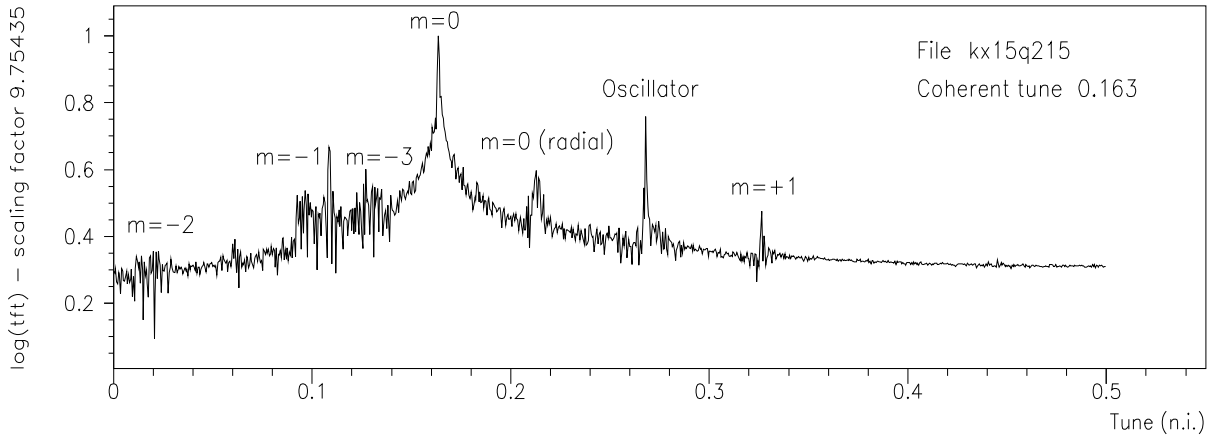


Figure 10: Transverse mode spectrum for $I_b=0.8$ mA, $Q_\beta=76.215$, $Q_f=0.295$, $K_x=-0.015\text{m}^{-1}$, showing the radial and the reflected modes.

By repeating the calculations for different values of Q_β and Q_f the curves of figure 11, representing the mode spectrum as function of the (zero-current) vertical tune, have been obtained: note the opposite slope of the curves corresponding to the (reflected) higher-order modes, as compared to those corresponding to the low-order modes. When the tune of mode $m=0$ becomes equal to that of mode $m=-3$, an instability occurs: this instability is related

to the feedback system, because theory predicts that in normal conditions mode $m=0$ should only couple with reflected modes of the same parity [9]. As a consequence, the machine and feedback settings will have to be chosen such as to prevent the tune of mode $m=0$ from getting too close to that of mode $m=-3$.

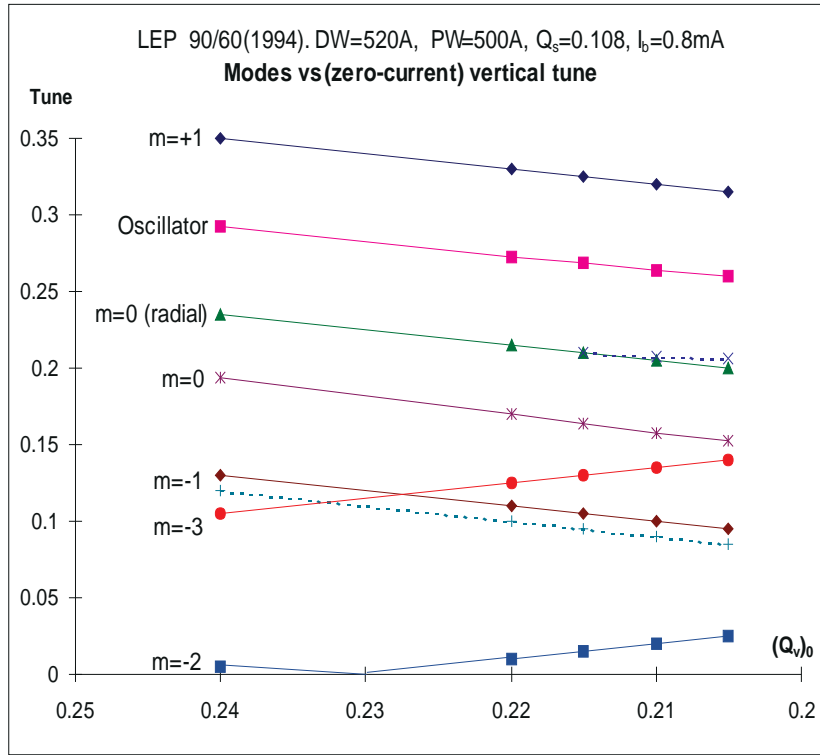


Figure 11: Instability due to coupling of the $m=0$ mode with the $m=-3$ (reflected) mode. $I_b=0.8$ mA, $K_x=-0.015\text{m}^{-1}$.

3.3 Maximum bunch current with feedback on

In this section, the capability of the feedback system to increase the maximum bunch current above the TMC limit will be studied. Figure 12 shows the results obtained with the oscillator tune set to $Q_f=0.32$, according to equation 2. For each current, a scan of the feedback gain has been carried out: since the compensation of the coherent detuning depends on the feedback gain, as a result of this calculation the stable tune range as function of current is obtained. The curve “ $m=0$ (minimum)” shows the position of the coherent tune corresponding to the minimum gain for which a stable beam is obtained; the curve “ $m=0$ (maximum)” is the one corresponding to the maximum gain. The curve labelled “Oscillator (minimum)” reports the position of the oscillator mode corresponding to the maximum gain: as the gain is reduced, the oscillator mode shifts to higher tunes.

As can be seen, the width of the stable tune range becomes smaller as the current is increased. For what concerns the lower limit, a possible interpretation of this result is the following: the “effective distance” in tune below which mode 0 and mode -1 can couple becomes

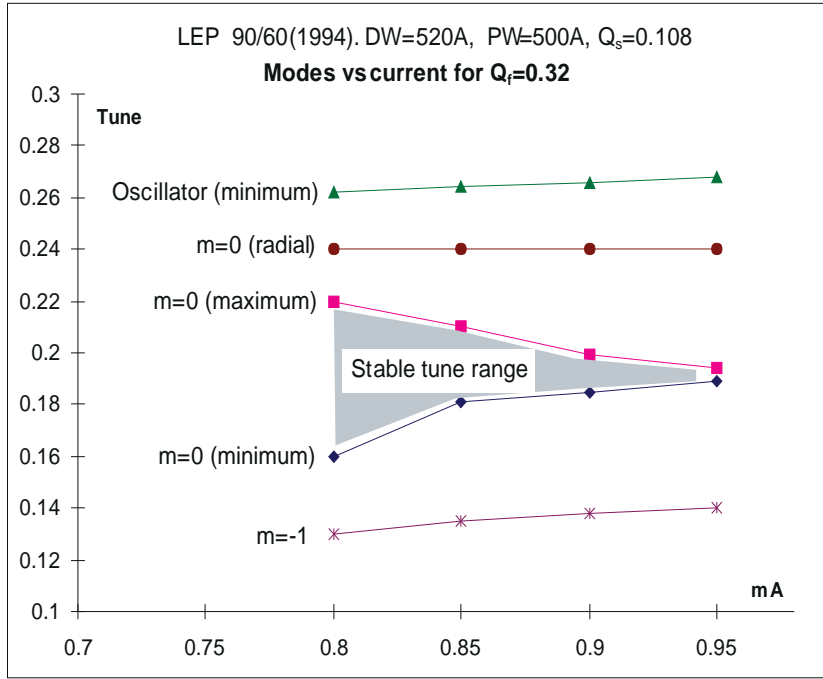


Figure 12: Stable tune range as function of current, and maximum current gain for $Q_f=0.32$.

larger as the current is increased. The positive slope of the “m=0 (minimum)” curve is also partly due to the positive tune shift with current of mode m=-1.

For what concerns the upper limit of the stable tune range, it is caused by coupling between the “oscillator” mode and the “m=0 (radial)” mode when their tunes get too close to each other (figure 6). In this case, however, it should be possible to overcome the limitation by shifting the (zero-coupling) oscillator tune Q_f to higher values. To check this, the calculation has been repeated with $Q_f=0.45$: as can be seen in figure 13, the “m=0 (maximum)” curve is now shifted up, the stable tune range is wider, and the current can be increased up to a value of 1.1 mA, corresponding to a current gain of 41% with respect to the TMC limit without feedback.

Figure 14 reports the simulation results for $I_b=1.1$ mA in an intermediate value of the stable tune range ($Q_{coh}=0.206$). With the new settings, the bunch current limitation is due to coupling between the different radial components of mode m=0. The transverse spectrum of figure 14 clearly shows the presence of new radial modes which appear for $I_b > 1$ mA and reduce the stable tune range in its upper part.

In conclusion, with one feedback oscillator used in the standard “attractive” mode of operation, and with the machine conditions which have been selected for the present study (in which the TMC limit was found to be 0.78 mA in simulation), the maximum gain in current can be estimated to be about 41%, leading to a maximum bunch current of 1.1 mA. This result, however, requires a fine tuning of the machine and feedback settings, and has been obtained in the hypothesis that no hardware limitations are present.

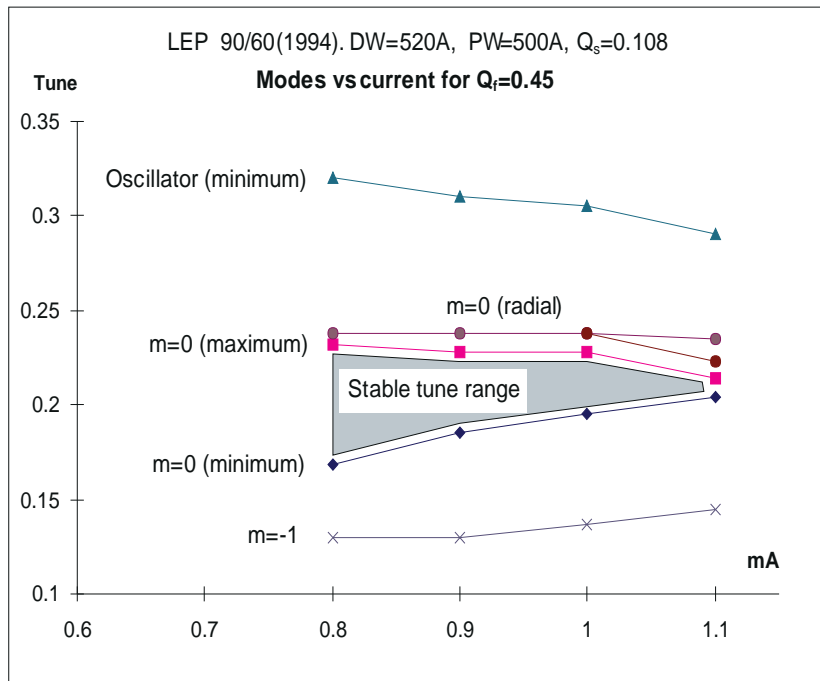


Figure 13: Stable tune range as function of current, and maximum current gain for $Q_f=0.45$.

INPUT FILE NAME pwhqhc (part 2) RUN DATE 11/ 8/ 95 TIME 9. 44. 18

Distributions are approximated by linear interpolation (20 ps step)
 Longitudinal wake switched ON – Transverse wake switched ON

Number of particles 2000 Damping time (s) 0.119 Beam energy (GeV) 20
 Number of turns 10000 Energy spread (MeV) 36.4 Radiation loss (MeV) 14.97

Bunch current (mA)	1.1	Betatron tune	76.24
Total RF Voltage (MV)	250	Synchrotron tune	0.108

FEEDBACK SETTINGS Phase advance between (virtual) pick-up and kicker (DEG) 0
 RMS pick-up noise (microns) 0 Number of kickers 1

Coupled-oscillator feedback switched on

First oscillator Tune 0.45 Gain (1/m) -0.25 Damping factor 1
 Second oscillator Tune 0 Gain (1/m) 0 Damping factor 1

Equilibrium values (averaged over 2000 turns)

Bunch center (ps) -90.9 Bunch length (ps) 42.433 Bunch width (mm) 0.144
 Mean energy (MeV) -6.288 Energy spread (MeV) 37.353 Total losses (MeV) 49.952

Total CPU time (s) 6736.96 Time for wake calculation (s) 439.988

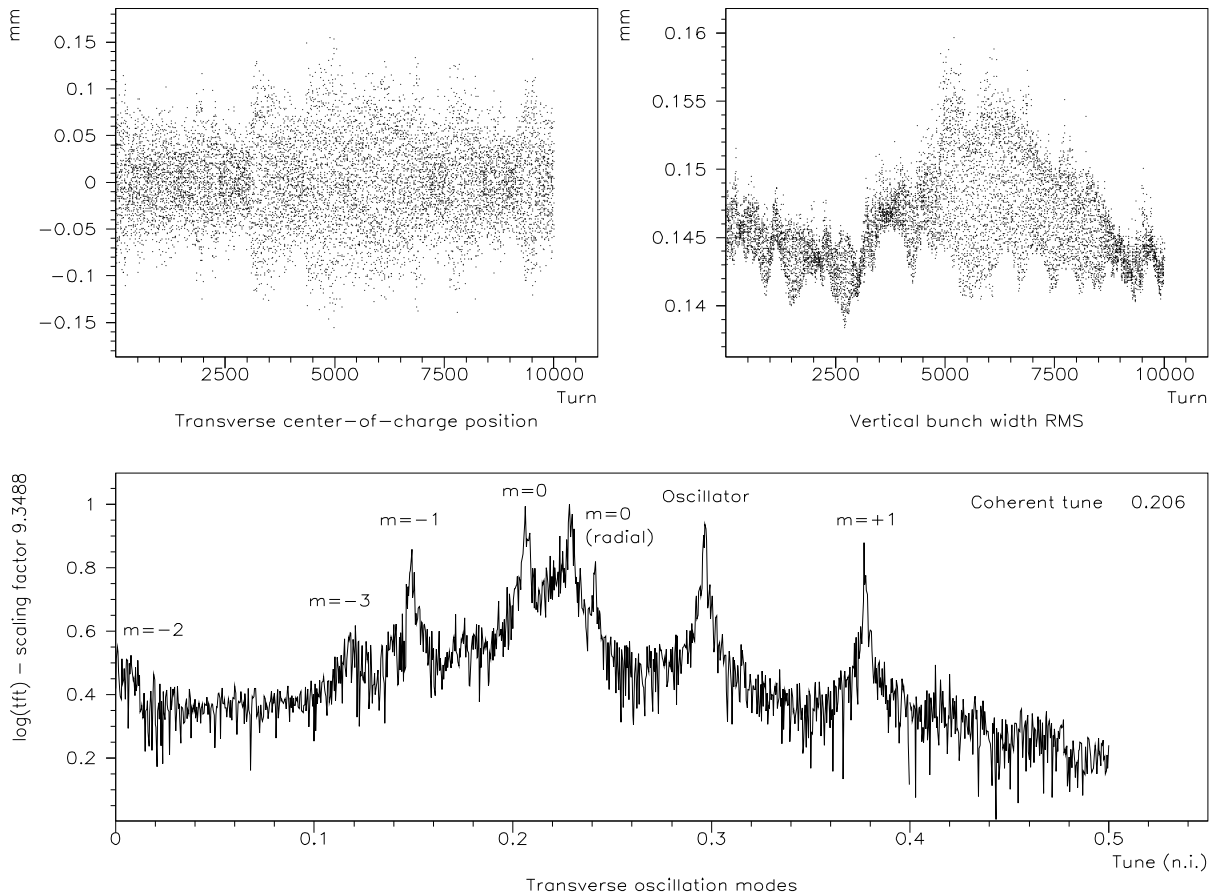


Figure 14: High bunch current with feedback.

4 Hardware limitations and damping of the feedback oscillator

The hardware limitations which affect the feedback performance are the accuracy of the pick-up system and the maximum deflection which can be delivered by the kicker. For what concerns the pick-up system, the main problems are the errors affecting the measurement of the bunch position at each pick-up, and the deviations of the pick-up gains g_1 and g_2 (equation 4) from a perfect setting, i.e. one corresponding to a zero-degree phase advance between the virtual pick-up and the kicker. As it was done in section 3, the analysis will be first carried out keeping a fixed bunch current of 0.8 mA, in order to achieve a good understanding of the system, and to study how to optimize the parameters, before addressing the question of the maximum current gain which can be achieved when hardware limitations are taken into account.

4.1 Pick-up noise

To study the effect of pick-up noise, a random component has been added to each position measurement. The random component has Gaussian distribution and user-defined RMS value. The calculations have been performed for noise levels between 1 and 10 μm RMS, which can be considered as typical values for high quality pick-ups. A first result of this calculation is illustrated in figure 15: as the noise level grows, the amplitude of the center-of-charge oscillation becomes proportionally larger, and the behaviour of the signal to noise ratio of the system is inherently stable.

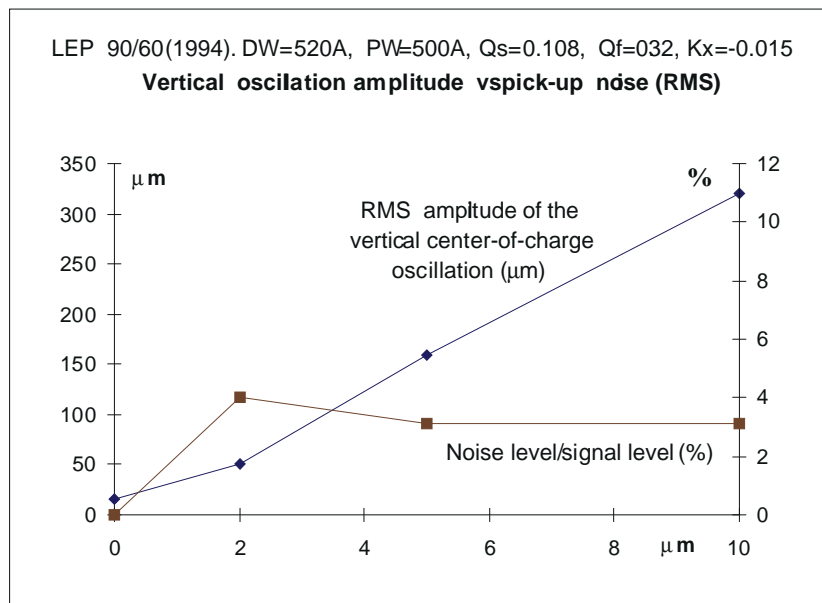


Figure 15: Dependence of the amplitude of the center-of-charge oscillation on the pick-up noise level.

A second result of the calculations is that as noise increases, the width of the peaks appearing in the bunch spectrum increases. This effect can be observed by comparing the spectrum of figure 16, corresponding to a noise of 5 μm RMS, with the one of figure 4, obtained with the same machine and feedback settings but with no pick-up noise.

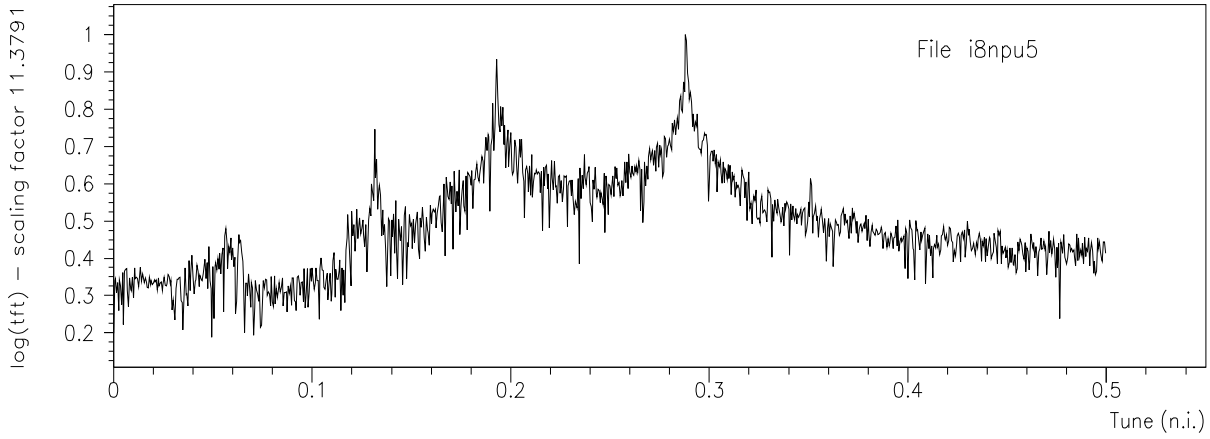


Figure 16: Broadening of the transverse mode spectrum due to pick-up noise. The RMS noise level is $5\mu\text{m}$; $I_b=0.8\text{ mA}$, $Q_f=0.32$, $K_x=-0.015\text{m}^{-1}$.

The broadening of the peaks in the spectrum can further reduce the available tune space, which has been shown to represent a critical aspect of the feedback system. This potential problem has been confirmed by a comparison between the results of calculations performed with a RMS noise level of $5\mu\text{m}$ and the ones obtained without noise: in the first calculation, performed with a bunch current of 0.8 mA , the maximum feedback gain allowed before reaching the instability due to coupling between the oscillator mode and the $m=0$ radial mode (figure 5) was found to be $K_x=-0.017\text{m}^{-1}$ instead of $K_x=-0.022\text{m}^{-1}$; in other terms, the instability occurs when the oscillator mode reaches a tune of 0.282 , while with no noise it can shift down to a tune of 0.262 . The second calculation was carried out for a fixed feedback gain of -0.015m^{-1} , and the current was increased until the onset of the instability due to coupling between mode 0 and mode -1 : the instability was reached for a bunch current of 0.85 mA and a coherent tune of 0.181 . A calculation performed in the same conditions but without pick-up noise reached the instability for a bunch current of 0.88 mA and a coherent tune of 0.176 .

4.2 Phase errors

The evaluation of the tolerance to deviations of the settings of the pick-up gains g_1 and g_2 (equation 4) from those corresponding to a phase advance of exactly zero degrees between the (virtual) pick-up and the kicker is essential in order to assess the feasibility of the feedback system: unfortunately, the simulations carried out for increasing values of the betatron phase advance $\Delta\theta$ between the virtual pick-up and the kicker (theoretically equal to zero) indicate a very high sensitivity of the system to this parameter: for a bunch current of 0.8 mA , a deviation of ± 0.2 degrees already leads to instability with a growth rate of about 60 ms (the damping time is $\tau_\epsilon=119\text{ ms}$); for a deviation of ± 0.5 degrees, the growth rate becomes about 30 ms . The bunch spectrum of figure 17 shows the anti-damping of mode $m=0$ for $\Delta\theta=0.2^\circ$, while figure 18 shows the anti-damping of the oscillator mode for $\Delta\theta=-0.2^\circ$: both spectra can be compared with the one of figure 4, obtained using the same machine and feedback settings, and with $\Delta\theta=0$. For lower bunch currents, smaller growth rates are obtained, but the requirements on the accuracy and stability of g_1 and g_2 remain extremely tight: at 0.4 mA , the growth rate of the instability is about 75 ms for a deviation of ± 0.5 degrees.

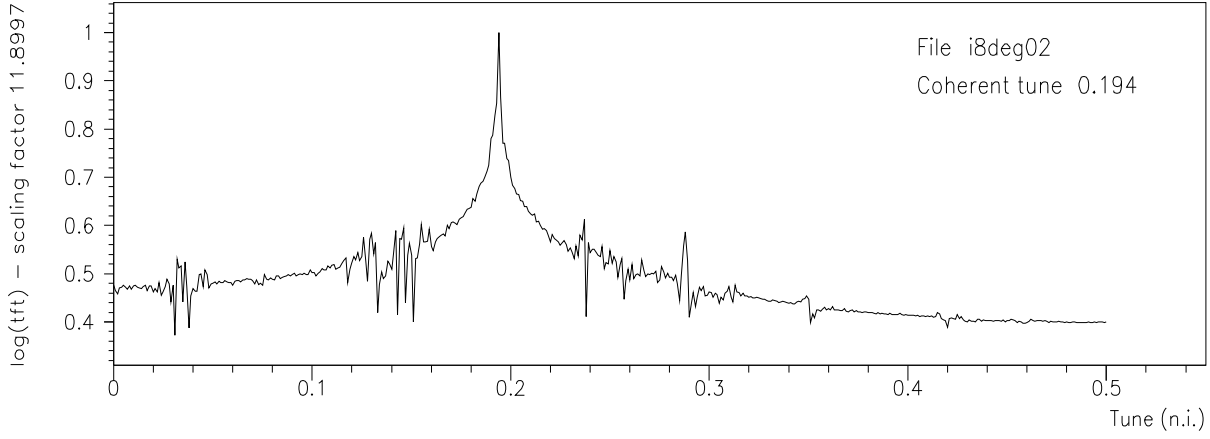


Figure 17: Anti-damping of mode $m=0$ for a phase advance of $+0.2^\circ$ between the virtual pick-up and the kicker. No noise on pick-ups, $I_b=800\mu\text{A}$, $Q_f=0.32$, $K_x=-0.015\text{m}^{-1}$.

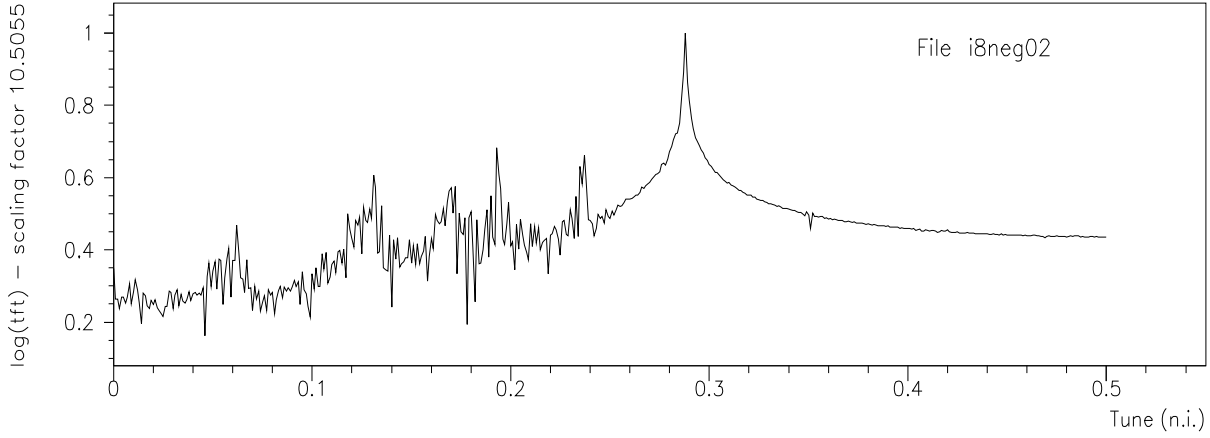


Figure 18: Anti-damping of the oscillator mode for a phase advance of -0.2° between the virtual pick-up and the kicker. No noise on pick-ups, $I_b=800\mu\text{A}$, $Q_f=0.32$, $K_x=-0.015\text{m}^{-1}$.

4.3 Damping of the feedback oscillator

After simulation studies indicated an unacceptable sensitivity of the feedback system with respect to phase errors, the original theory was revised by V. Danilov and E. Perevedentsev by introducing a damping factor d in the oscillator equation:

$$\begin{bmatrix} x \\ x' \end{bmatrix}_{k+1} = \begin{bmatrix} \cos \mu_f & \sin \mu_f \\ -d \sin \mu_f & d \cos \mu_f \end{bmatrix} \begin{bmatrix} x \\ x' \end{bmatrix}_k \quad (5)$$

This results in damping of the oscillator mode, allowing for a stable bunch in a wider interval of (negative) $\Delta\theta$. However, theory also predicted that the damping factor on the feedback oscillator may cause anti-damping of other modes: for this reason, the damping factor must remain within a window of values such that none of the relevant modes is anti-damped to rates higher than the radiation damping rate.

The possibility of decreasing the sensitivity of the feedback system with respect to phase errors by damping the feedback oscillator is confirmed by a series of calculations carried out with $I_b=0.8\text{ mA}$ and $\Delta\theta=-5^\circ$: the results show that the bunch remains stable for $0.85 < d < 0.9$. The

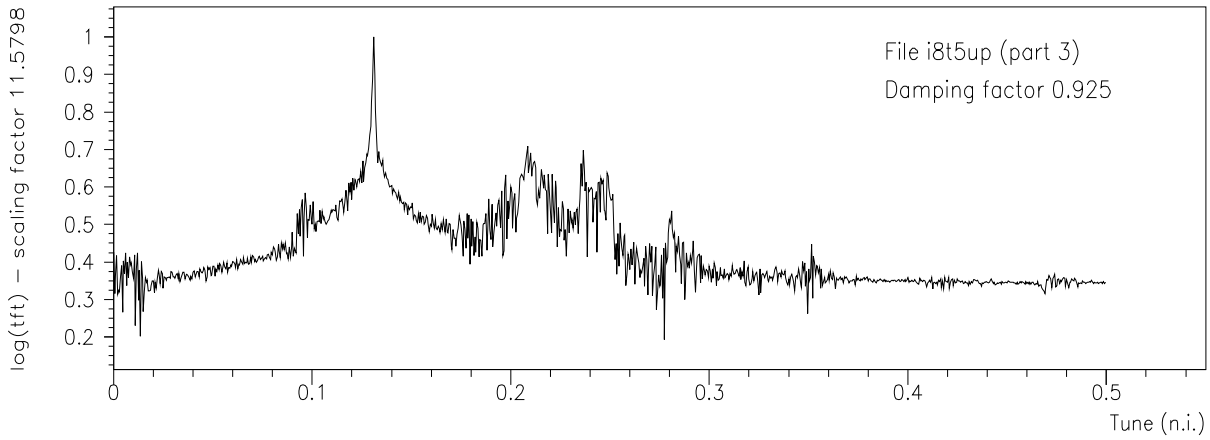


Figure 19: Anti-damping of mode $m=-1$ for $\Delta\theta=-5^\circ$ and $d = 0.925$. $I_b=800\mu\text{A}$, $Q_f=0.32$, $K_x=-0.015\text{m}^{-1}$. No noise on pick-ups.

instability due to anti-damping of mode $m=-1$ could be clearly observed for $d = 0.925$ (figure 19), while for $d < 0.85$ it is mode $m=0$ which becomes unstable.

Since it is difficult to predict the optimal value for the damping factor d on the basis of theoretical considerations, the interval of d values which provide a stable bunch has been studied as function of the phase shift $\Delta\theta$, for $I_b=0.8$ mA. As can be seen in figure 20, it is possible to obtain a stable beam for $-8^\circ < \Delta\theta < 0^\circ$. The width of the stable area gives an indication of the stable phase range as function of d : a maximum width of about 2° is obtained for $0.91 < d < 0.96$.

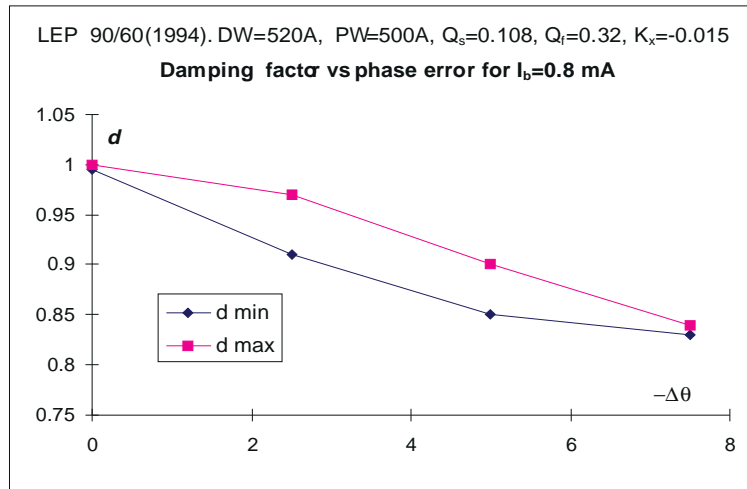


Figure 20: Stable range for the damping factor d as function of the phase error $\Delta\theta$.

Figure 21 reports the results obtained for the stable phase range as function of current, for $d=0.94$ and $Q_f=0.45$. The feedback gain for the different currents has been chosen on the basis of the results reported in figure 13, keeping the coherent tune in the central region of the stable tune range. As can be seen, the damping factor on the feedback oscillator allows for rather large phase errors at low current; however, the accuracy and stability of the phase becomes critical as the current is increased: at 1 mA, the stable range for $\Delta\theta$ was found to be about

¹. It should be noted that the optimal value for the damping factor d has been determined for a current of 0.8 mA, and has not been optimized as function of current: however, since the curves of figure 20 show that the width of the stable phase range is essentially constant for $0.91 < d < 0.96$, it is not expected that such optimization would result in a big improvement of the results presented in figure 21.

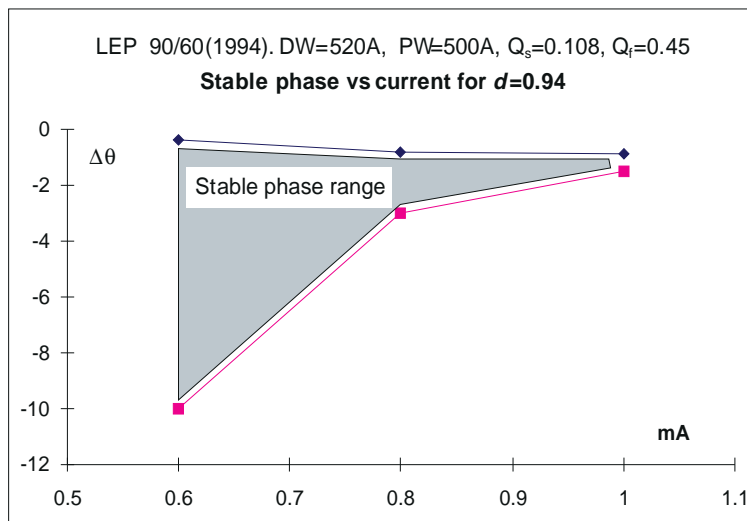


Figure 21: Stable phase range as function of current for $d=0.94$.

4.4 Maximum bunch current with phase errors and noise

The results presented in the previous sections indicate that, with the machine configuration and feedback settings which have been considered, the coupled-oscillator feedback system can achieve a substantial current gain only if the hardware can meet tight specifications in both accuracy and stability: the calculations carried out for $I_b=1$ mA (corresponding to a 25% gain in current, and a 50% gain in luminosity) and with $d=0.94$ show that the phase range allowed is $-1.5^\circ < \Delta\theta < -0.7^\circ$ for a pick-up noise of $2 \mu\text{m}$ RMS. At $\Delta\theta=-1^\circ$, the maximum pick-up noise allowed before particles are lost is $3 \mu\text{m}$ RMS. Figure 22 reports the simulation results for a phase deviation of -1° and a RMS pick-up noise of $2 \mu\text{m}$. For what concerns the accuracy required on the feedback settings, it was found that in the conditions of the calculation reported in figure 22, the stable range for the feedback gain is $-0.1775\text{m}^{-1} < K_x < -0.1625\text{m}^{-1}$, corresponding to a relative variation of 8%. The corresponding range of variation for the coherent tune of mode $m=0$ is $0.199 < Q_{coh} < 0.206$. For $K_x=-0.17\text{m}^{-1}$, the stable range for the oscillator tune is 0.007, from $Q_f=0.444$ to $Q_f=0.451$. For what concerns the constraints on the kicker system, in the conditions of the calculation reported in figure 22, the kick strength required would be $3 \mu\text{rad}$ for a β value of 56.4 m at the kicker². For fixed machine and feedback settings, the kick strength required increases rather rapidly with the noise level (see section 5); according to the design specifications, the kicker magnets of the LEP transverse feedback can deliver angular deflections up to $8 \mu\text{rad}$ [10]; the vertical β function at their location is about 110 m.

²The kick strength required scales as the inverse of the square root of β_{kicker} .

INPUT FILE NAME imxp1n2 (part 1) RUN DATE 20/ 8/ 95 TIME 14. 32. 42

Distributions are approximated by linear interpolation (20 ps step)
 Longitudinal wake switched ON – Transverse wake switched ON

Number of particles 2000 Damping time (s) 0.119 Beam energy (GeV) 20
 Number of turns 10000 Energy spread (MeV) 36.4 Radiation loss (MeV) 14.97

Bunch current (mA)	1	Betatron tune	76.24
Total RF Voltage (MV)	250	Synchrotron tune	0.108

FEEDBACK SETTINGS Phase advance between (virtual) pick-up and kicker (DEG) -1
 RMS pick-up noise (microns) 2 Number of kickers 1

Coupled-oscillator feedback switched on

First oscillator Tune 0.45 Gain (1/m) -0.17 Damping factor 0.94
 Second oscillator Tune 0 Gain (1/m) 0 Damping factor 1

Equilibrium values (averaged over 2000 turns)

Bunch center (ps) -85.361 Bunch length (ps) 41.827 Bunch width (mm) 0.174
 Mean energy (MeV) -5.908 Energy spread (MeV) 36.79 Total losses (MeV) 46.946

Total CPU time (s) 1660.46 Time for wake calculation (s) 109.955

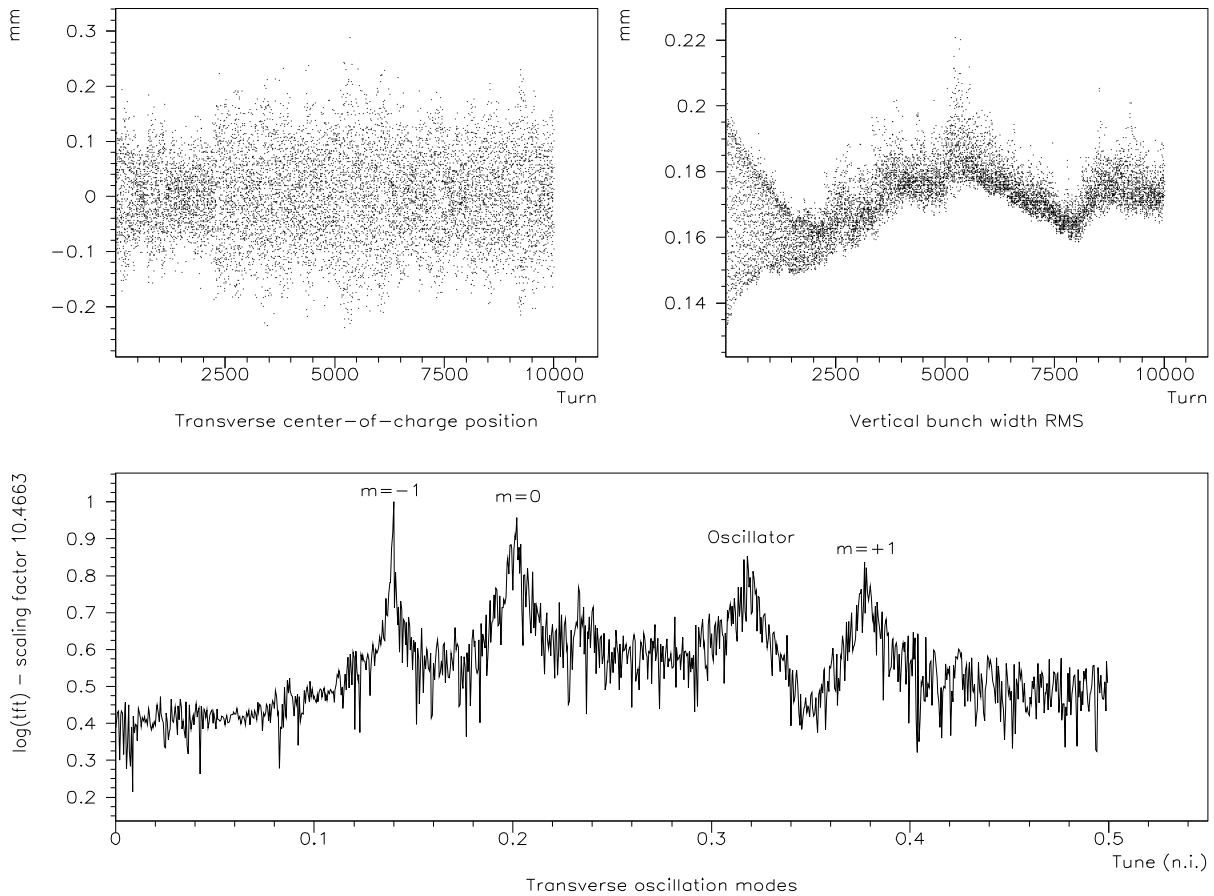


Figure 22: Simulation results for $I_b=1\text{mA}$.

5 Feedback operation in “repulsive” mode

The main purpose of a feedback system counteracting the transverse mode coupling instability is to compensate the coherent detuning of the $m=0$ mode, in order to prevent its tune from approaching that of mode $m=-1$. In the configurations which have been studied in the previous sections, the coupled-oscillator feedback system achieves this goal by producing an attractive force between mode $m=0$ and an oscillator placed in the upper part of the spectrum. However a repulsive force may also be produced: for this, it is sufficient to invert the sign of the gain. In this configuration, however, a damping factor on the oscillator is required even if the pick-up gains provide a phase setting of exactly zero degrees, in order to avoid anti-damping of mode $m=0$ (figure 23); at the same time, a too strong damping of the oscillator results in anti-damping of mode $m=-1$ (figure 24).

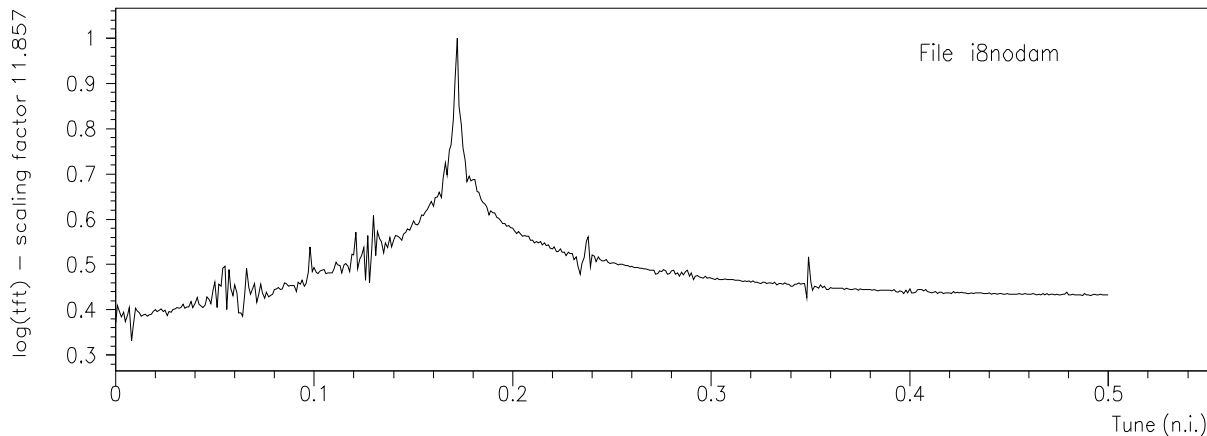


Figure 23: Anti-damping of the mode $m=0$ for $\Delta\theta=0^0$ and $d=1$. $I_b=0.8$ mA, $Q_f=0.11$, $K_x=0.003\text{m}^{-1}$. Operation in repulsive mode, no noise on pick-ups.

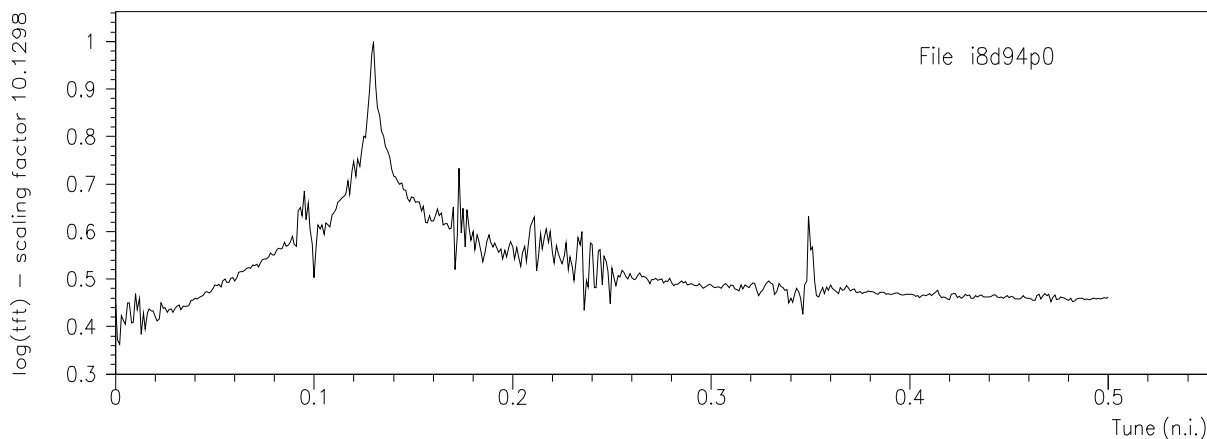


Figure 24: Anti-damping of mode $m=-1$ for $\Delta\theta=0^0$ and $d=0.94$. $I_b=0.8$ mA, $Q_f=0.11$, $K_x=0.003\text{m}^{-1}$. Operation in repulsive mode, no noise on pick-ups.

The operation in “repulsive” mode can be expected to improve the stability of the system as compared to the operation in “attractive” mode: in fact, since the intensity of the coupling force between the oscillator and the dipole mode increases as their frequencies approach each

other, when the tune of mode $m=0$ shifts down due to the coherent force and approaches the synchrotron sideband $m=-1$ a higher repulsive force is automatically produced. Unfortunately, no studies of the properties of the feedback system using a single repulsive oscillator placed in the lower part of the spectrum have been carried out so far, either in former simulation studies or during the machine experiments: *the results presented in this section indicate that the configurations based on a single oscillator should be further investigated before deciding to upgrade the feedback system by adding a second oscillator, as it was previously planned [2].*

The simulations carried out using the coupled-oscillator feedback in repulsive mode indicate that several advantages are present. The first advantage is *an increased tolerance with respect to pick-up noise*: figure 28 shows the results obtained for a bunch current of 1 mA and a pick-up noise levels of $5 \mu\text{m}$ RMS; in fact, the beam was found to remain stable also for higher noise levels. Up to $10 \mu\text{m}$ RMS no particles are lost, but the transverse dimension of the bunch steadily increases with noise, and shows an oscillatory behaviour with bumps of increasing amplitude. For an RMS noise of $15\text{-}20\mu\text{m}$ RMS, the particles with the largest amplitude of oscillation are lost when the bump reaches its maximum. Figure 25 shows the oscillatory behaviour of the vertical bunch width in the same conditions of figure 28, but with a pick-up noise of $20\mu\text{m}$ RMS. In the attractive mode, a similar behaviour is observed (figure 22), but particles are lost already for a noise level of $4\mu\text{m}$ RMS.

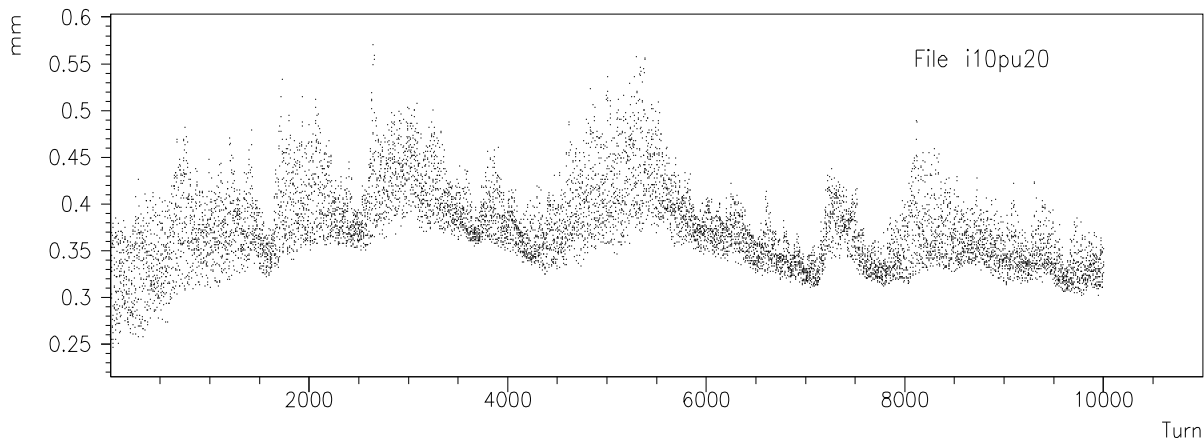


Figure 25: Vertical size bumps with a pick-up noise of $20\mu\text{m}$ RMS.

For what concerns the *range of stability with respect to the choice of the feedback parameters*, the following results were obtained: for a bunch current of 1 mA, an oscillator tune $Q_f=0.11$, and a pick-up noise level of $5 \mu\text{m}$ RMS, the gain could be varied from 0.012m^{-1} up to 0.017m^{-1} (corresponding to a relative variation of 40%), while for a fixed feedback gain of 0.015m^{-1} , the oscillator tune could be varied from $Q_f=0.10$ (figure 26) to $Q_f=0.12$ (figure 27), corresponding to a tune space of 0.02. In the attractive mode, with a lower noise level of $2\mu\text{m}$ RMS, the maximum allowed variation of the gain was 8%, and the tune space for the oscillator was 0.007. The width of the stable range for the coherent tune of mode $m=0$ was 0.012 in the repulsive mode and 0.007 in the attractive mode.

Unfortunately, for what concerns the *stability with respect to phase errors*, the repulsive mode of operation showed, so far, limitations similar to those observed with the attractive mode: with $d=0.99$ and a noise level of $5 \mu\text{m}$ RMS, the stable phase range is $-0.5^\circ < \Delta\theta < 0.25^\circ$;

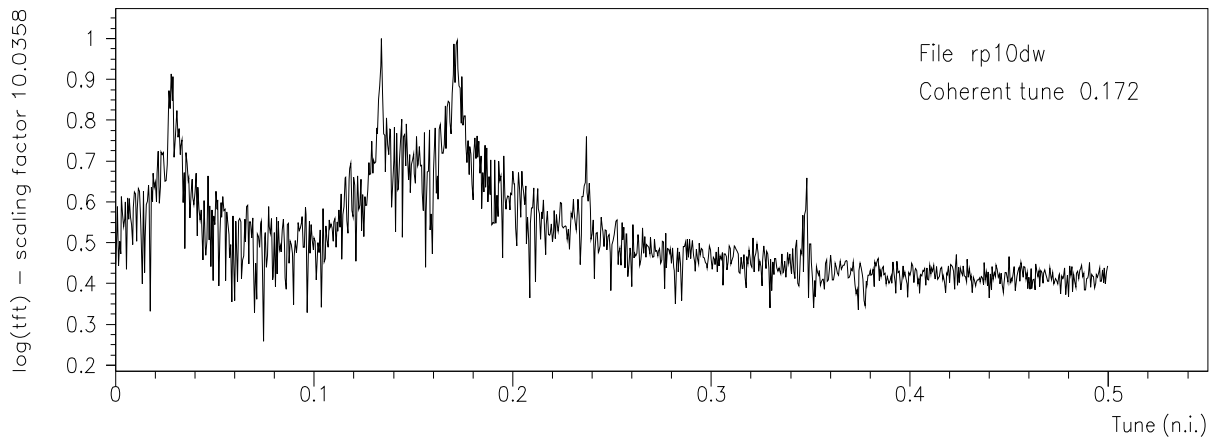


Figure 26: Vertical bunch spectrum for $Q_f=0.10$ and $K_x=0.015\text{m}^{-1}$. The other settings are the same as in figure 28.

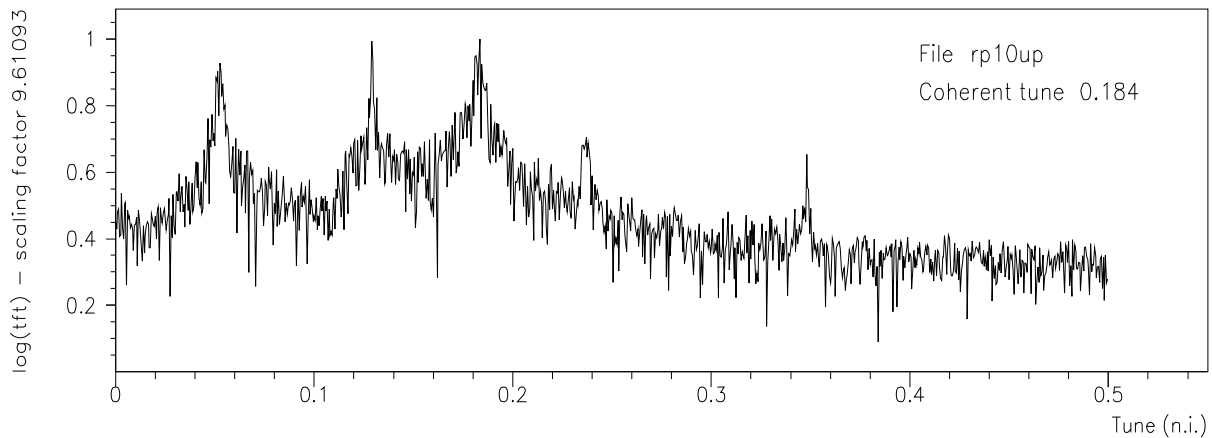


Figure 27: Vertical bunch spectrum for $Q_f=0.12$ and $K_x=0.015\text{m}^{-1}$. The other settings are the same as in figure 28.

with stronger damping, the stable phases shift to larger values, but the width of the stable phase range is not increased.

In the conditions of figure 28, with a pick-up noise of $5\mu\text{m}$ RMS, the *kick strength* required is $4.4\mu\text{rad}$ for a β of 56.4 m at the kicker (it scales as the inverse of the square root of β_{kicker}). The kick strength required depends on pick-up noise: at $10\mu\text{m}$ RMS, deflections up to $11\mu\text{rad}$ would be required. Since the kicker magnets of the present feedback system for LEP can deliver angular deflections up to $8\mu\text{rad}$ and are placed at $\beta=110\text{ m}$ [10], they would limit the performance only for noise levels in excess of $10\mu\text{m}$ RMS.

INPUT FILE NAME i10pu5 (part 1) RUN DATE 22/ 8/ 95 TIME 12. 18. 20

Distributions are approximated by linear interpolation (20 ps step)
 Longitudinal wake switched ON – Transverse wake switched ON

Number of particles 2000 Damping time (s) 0.119 Beam energy (GeV) 20
 Number of turns 15000 Energy spread (MeV) 36.4 Radiation loss (MeV) 14.97

Bunch current (mA)	1	Betatron tune	76.24
Total RF Voltage (MV)	250	Synchrotron tune	0.108

FEEDBACK SETTINGS Phase advance between (virtual) pick-up and kicker (DEG) -0.1
 RMS pick-up noise (microns) 5 Number of kickers 1

Coupled-oscillator feedback switched on

First oscillator Tune 0.11 Gain (1/m) 0.015 Damping factor 0.99
 Second oscillator Tune 0 Gain (1/m) 0 Damping factor 1

Equilibrium values (averaged over 2000 turns)

Bunch center (ps) -84.942 Bunch length (ps) 42.375 Bunch width (mm) 0.156
 Mean energy (MeV) -5.883 Energy spread (MeV) 37.251 Total losses (MeV) 46.718

Total CPU time (s) 2557.01 Time for wake calculation (s) 172.205

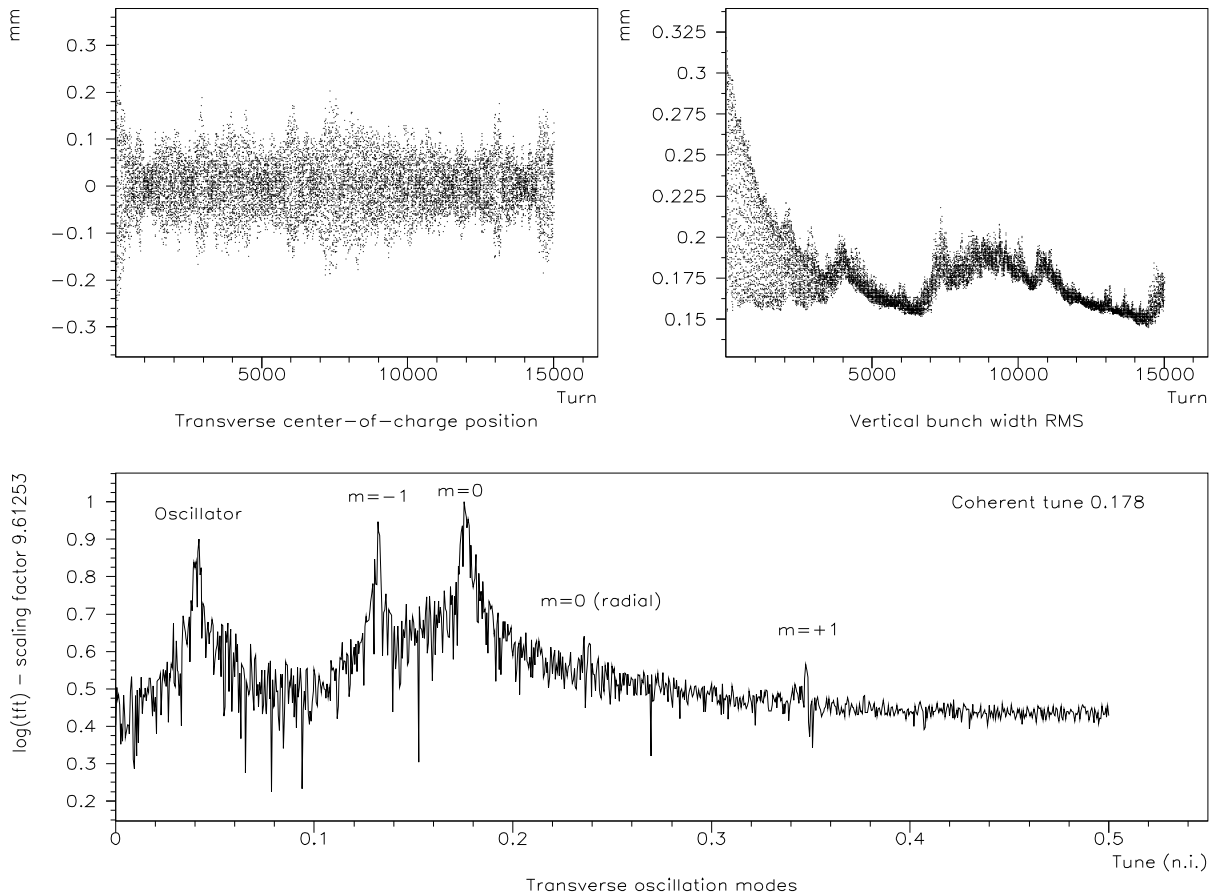


Figure 28: High current with the feedback system operating in repulsive mode.

6 Conclusions

Some results obtained by simulating the collective motion of a LEP bunch in the presence of coupled-oscillator feedback systems counteracting TMC have been presented. For bunch currents comparable to the threshold for transverse mode coupling, simulation results confirmed the theoretical predictions concerning the capability of the feedback system to compensate the coherent detuning of mode $m=0$; however, as the current is increased above the TMC limit, the tune space is progressively reduced and the choice of the feedback parameters becomes more critical. In the conditions chosen for the present study (damping and polarization wigglers at nominal settings, $Q_s=0.108$, $Q_\beta=76.24$), the TMC limit was found to be 0.78 mA in simulation³: using one feedback oscillator in the attractive mode of operation, after a careful optimization of the settings the maximum current gain was found to be about 40% ($I_b^{max}=1.1$ mA) if no hardware limitations are taken into account.

The hardware limitations which affect the system performance are pick-up noise, phase errors, and maximum kick strength. Pick-up noise was shown to cause a broadening of the peaks in the transverse spectrum, resulting in further reduction of the available tune space; besides this, the kick strength required increases rather rapidly with pick-up noise. Small phase errors were shown to result in instabilities already at low currents; however, the possibility of decreasing this sensitivity by damping the feedback oscillator was also demonstrated. At low current, the feedback system with damping can tolerate rather large phase errors, but as the current increases the maximum deviation allowed is progressively reduced. According to simulation, with the machine conditions which have been selected for the present study, and with the feedback system used in the attractive mode of operation, in order to reach a 25% current gain with respect to the TMC limit (50% gain in luminosity) the hardware should meet the following specifications:

- Stable phase range: 0.8° .
- Stable tune range for the oscillator: 0.007.
- Maximum (relative) variation for the feedback gain allowed: 8%.
- Pick-up noise: below $3\mu\text{m}$ RMS.
- Kick strength: angular deflections of $3\mu\text{rad}$ are needed for a noise level of $2\mu\text{m}$ RMS and a β of 56.4 m at the kicker⁴.

The first two requirements would be very difficult to comply with; for what concerns the other constraints, a position measurement with an accuracy below $3\mu\text{m}$ RMS can be achieved with present technology but requires high quality pick-ups, while the necessary kick strength would be within the specifications of the kicker magnets presently installed at LEP.

The first machine development session dedicated to the new feedback system was carried out in 1993 without the support of simulation studies, and was not successful: although some positive tune shift could be briefly observed, the beam became systematically unstable as soon as the feedback system was switched on. With better insight obtained from simulation studies performed in 1994 [2] a second experiment was carried out, using improved parameters and damping on the feedback oscillator: the system behaviour was found to correspond very closely to what had been observed in simulation [2].

³During a machine experiment carried out in similar conditions, the threshold current was found to be 0.73 mA.

⁴The kick strength required scales as the inverse of the square root of β_{kicker} .

The simulations presented in section 3 and 4, and both the experimental tests, were carried out using the feedback system with a single oscillator used in attractive mode; in section 5, an alternative repulsive mode of operation for the single-oscillator configuration has been considered: simulation results indicate that in this mode of operation some relaxation of the hardware constraints for a 25% current increase is possible:

- Stable tune range for the oscillator: 0.02.
- Pick-up noise: below $10\mu\text{m}$ RMS.
- Maximum (relative) variation for the feedback gain allowed: 40%.
- Kick strength (for a β value of 56.4 m at the kicker, see also footnote): $4.7\mu\text{rad}$ for a pick-up noise of $5\mu\text{m}$ RMS and $11\mu\text{rad}$ for a pick-up noise of $10\mu\text{m}$ RMS.

However, no improvement was observed so far for what concerns the tolerance to phase errors, which represents the main problem still to be solved. It should be noted, however, that the analysis reported here is not exhaustive, and that new strategies in the choice of the machine and feedback settings may result in better tolerances and larger current gains: studies in this direction are currently under way, and the possibility of obtaining a more efficient and flexible system by introducing a second feedback oscillator is also considered.

ACKNOWLEDGEMENTS

I would like to thank Bruno Zotter for the constant support, encouragement and friendship he gave me during my stay at CERN. I would also like to thank all the members of the AP group, in particular Jacques Gareyte, for their kind hospitality.

References

- [1] V. Danilov, E. Perevedentsev, “*Feedback system for elimination of the transverse mode coupling instability*”, CERN SL/93-38 (AP), September 1993.
- [2] D. Brandt, “*What is new on the (transverse) feedback front?*”, Proceedings of the fifth workshop on LEP performance, Chamonix, January 1995.
- [3] G. Sabbi, “*TRISIM User’s Guide*”, CERN SL/94-73 (AP), August 1994.
- [4] G. Sabbi, “*Simulation of single-bunch collective effects in LEP by linear expansion of the distribution moments*”, CERN SL/95-25 (AP), May 1995.
- [5] Y.H. Chin, “*ABCI User’s Guide*”, LBL Report 33091, 1992.
- [6] G. Sabbi, “*LEP beam parameters at injection as function of wiggler excitation*”, CERN SL Note 95-70 (AP), May 1995.
- [7] G. Sabbi, A. Wagner, “*Single-bunch intensity limitations in low-emittance lattices for LEP*”, CERN SL/95-70 (AP).
- [8] E. Perevedentsev, private communication.
- [9] F. Ruggiero, “*Theoretical aspects of some collective instabilities in high-energy particle storage rings*”, CERN 86-06, Lep Main Ring Division, August 8, 1986.
- [10] E. Peschardt, private communication.